

Growth of Fractally Rough Colloids

K. D. Keefer and D. W. Schaefer

Sandia National Laboratories, Albuquerque, New Mexico 87185

(Received 20 December 1985)

We report the growth and structure of fractally rough silicate particles in solution. Using small-angle x-ray scattering, we find fractal surfaces both in solution and in a porous solid made from the solution precursor. Finally, we develop a simple model which both is consistent with silicate chemistry and generates fractally rough structures.

PACS numbers: 68.70.+w, 61.10.Lx, 82.70.Dd, 82.70.Rr

It is not at all obvious that objects which grow in an indeterminate fashion can have characteristic statistical structures. Yet one of the most interesting phenomena in random growth is that systems with only short-range forces and no long-range order can form particles whose large-scale structure is both distinctive and statistically well defined. Many of these structures can be described as mass fractals,¹ objects whose mass (M) scales as their radius (R) to a power (D) less than the dimension of space (d): $M \propto R^D$, $1 < D < d$.

In contrast to mass fractals, we report a system which produces a different class of objects: homogeneous colloidal particles with fractally rough surfaces. We not only demonstrate the growth of fractally rough particles, but also show that a solid with fractal porosity can be made from the rough particles. Finally, a simple model is developed which incorporates only local chemistry and yet generates fractally rough clusters in two dimensions.

Although several groups find evidence for fractal surfaces in solids,²⁻⁴ we believe that our study is the first to demonstrate the growth of surface fractals and the first to explain the origin of fractal surfaces in terms of random growth. These fractally rough colloids grow in solutions of partially hydrolyzed silicon tetraethoxide [$\text{Si}(\text{OC}_2\text{H}_5)_4$, TEOS]. Silicate species grown in such solutions can have a particularly diverse range of random structures, from weakly cross-linked polymers⁵ to dense, smooth colloidal particles.⁶ The class of structures we produce is of interest both because of the unique growth process and because of the potential technological importance of the new class of surface structures.

Surface fractals are objects whose mass scales as the radius in a Euclidian fashion ($D = d$), but whose surface area, S (measured with a fixed "yard stick" or tile size), increases with radius more rapidly²:

$$S \propto R^{D_s}, \quad d-1 \leq D_s \leq d. \quad (1)$$

Equation (1) is obeyed only over a limited range of length scales. At large length scales (beyond a "surface correlation range") the object becomes uniform so that $D_s \rightarrow d-1$ ($=2$ for $d=3$). On short length scales, the objects either may become smooth

($D_s \rightarrow 2$) or may reflect the short-range chemical configurations. If the object is rough on length scales comparable to its radius, then it reduces to a mass fractal of dimension D . A mass fractal is therefore a surface fractal which is rough on all length scales and whose surface area scales with the mass ($1 \leq D_s = D \leq d$).

Scattering experiments, both small-angle x ray (SAXS) and light, are the techniques of choice for structure determination. Mass fractals give rise to power-law scattering curves in the intermediate or Porod regime⁷⁻⁹:

$$I(K) \sim K^{-D}, \quad 1 \leq D < 3, \quad (2)$$

where $K = 4\pi(\sin\theta)/\lambda$, 2θ is the scattering angle, and λ is the wavelength of the radiation. If an object is uniform (i.e., $D=3$), the scattering also generates a power-law profile³ which depends on the structure of the surface:

$$I(K) \sim K^{D_s-6}; \quad d-1 < D_s < d. \quad (3)$$

For uniform objects with smooth, nonfractal surfaces, $D_s=2$ and Eq. (3) gives the familiar Porod's law ($I \sim K^{-4}$). Equation (3) is therefore a generalization of Porod's law for fractal surfaces. Scattering measurements can distinguish between mass fractals (scattering exponents of -1 to -3) and surface fractals (exponents of -3 to -4).⁴

Two x-ray instruments were used in the study. The solution work was done with a Kratky system whereas the porous solid was studied with a pinhole camera. Because of the smearing effect of line geometry, the data from the Kratky system must be desmeared before comparison to Eqs. (2) and (3). For power-law profiles, however, the observed smeared intensity profile is just $KI(K)$ so the curves are analytically desmeared by dividing the observed intensity by K . This procedure is inadequate outside power-law regions. As a control, we also measured dense colloidal silica (Ludox SM) and found Porod-law behavior, $I(K) \sim K^{-4}$, in the analytically desmeared data.⁸

The silica solutions were prepared by hydrolysis of TEOS at room temperature in alkaline (0.01M NH_4OH) ethanol solutions with $\text{H}_2\text{O}:\text{TEOS}$ ratios, W ,

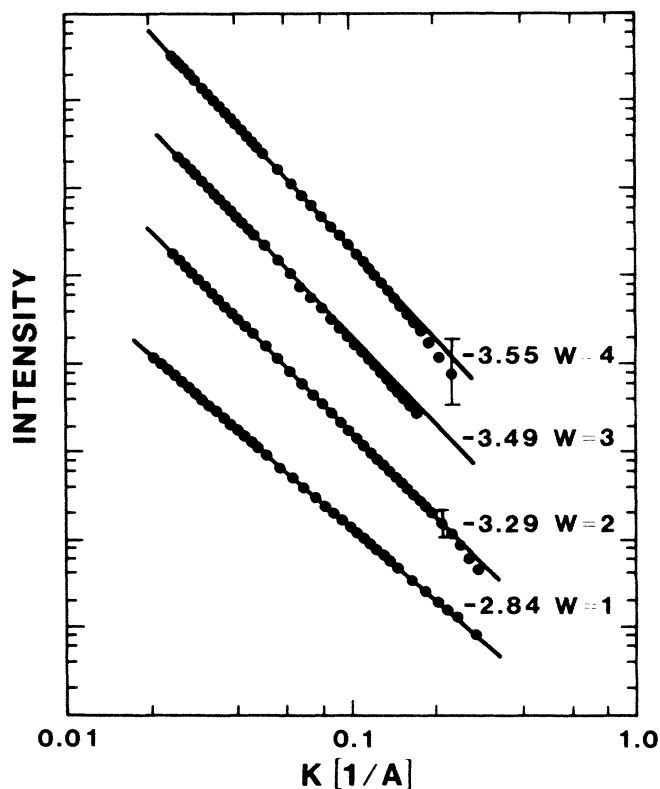


FIG. 1. Scattering profiles from silicate polymers grown in alkaline solution as a function of the molar ratio, $W = \text{H}_2\text{O}/\text{Si}$. Note that all data points shown are used in determination of the properly weighted linear least-square fit. Data were analytically desmeared to give the pinhole equivalent curves. Initial concentration of NH_4OH is $0.01 M$. Data are taken eight days after the initiation of the reaction.

of 1 to 4. After 190 h, the x-ray scattering from these solutions was measured (Fig. 1). The scattering from the solution with $W=1$ yields an exponent of -2.8 which we interpret as a mass fractal. For the solutions with $W=2, 3,$ and 4 , the scattering curves exhibit a decade of power-law behavior with scattering exponents which change continuously from -3.3 to -3.6 as the water ratio increases from 2 to 4. We interpret the exponents as arising from surface fractals. Since there is no discontinuity in the chemistry of the system, this scattering behavior suggests that the system is crossing over from mass- to surface-fractal behavior. The data could also be interpreted as scattering from power-law polydisperse distribution of particles, as discussed below.

We also studied the structure of a porous solid

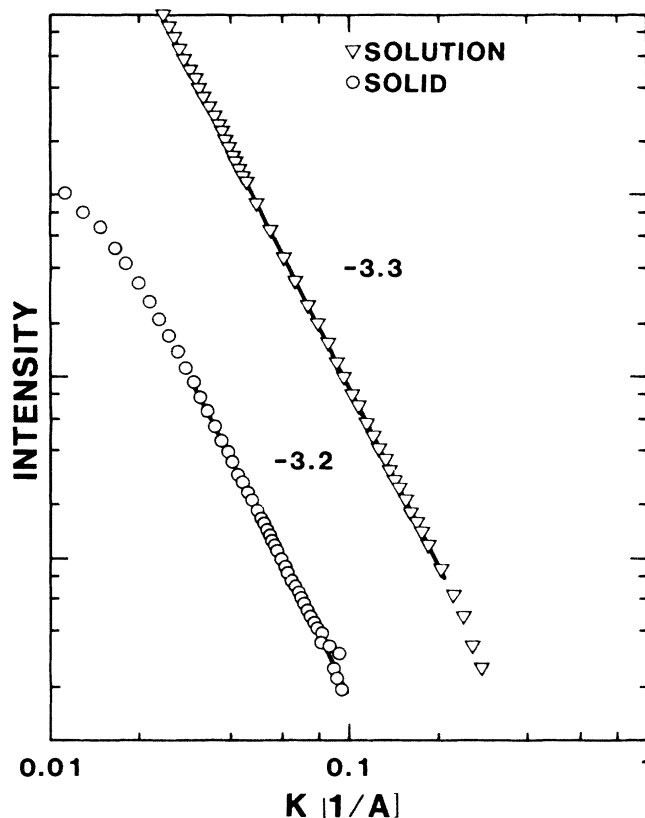
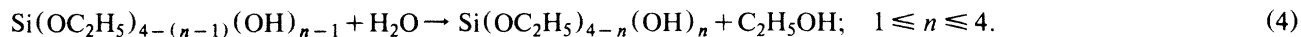


FIG. 2. Comparison of the $W=2$ solution scattering curve with that of a porous solid made by air drying of the solution.

prepared by air drying of the $W=2$ sample in Fig. 1. Figure 2 compares the scattering profiles of the translucent solid to its solution precursor. At large K , the curves are nearly identical, indicating that the surface-fractal character of the precursor is retained in the solid. The curvature near $K=0.02 \text{ \AA}^{-1}$ suggests that the structure is uniform over distances larger than $\sim 50 \text{ \AA}$. This length is related to the mean pore radius, but the detailed shape in the crossover region is unknown.

On the basis of silicate chemistry, we develop a simple growth model which generates fractally rough particles. Having established a reasonable growth model, we then discuss its consequences, including the classes of structure which can be grown, and the effect of polydispersity.

In our system, silica condensation polymerization proceeds by a two-step process. In the first step, functional sites ($-\text{SiOH}$ groups) are generated by the hydrolysis of noncondensable alkoxide groups¹⁰:

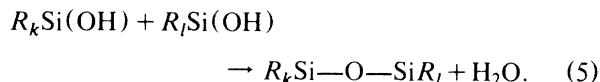


The silicate species on the right-hand side of Eq. (4) is an " n functional" monomer which can form $n \text{ Si-O-Si}$ linkages by condensation (see below).

In basic solution, reaction (4) proceeds by a nucleophilic substitution mechanism^{6,10} which (1) inverts the sili-

cate molecule, and (2) becomes more facile as n increases. Because of the inversion, hydrolysis becomes more difficult once a monomer is incorporated into a cluster. Unhydrolyzed sites on polymers are thereby "poisoned" and do not polymerize readily. Because of item (2) above, a nonuniform distribution of monomers develops and the system can become depleted in monomers of intermediate ($n \sim 3$) functionality. These two factors, coupled with a third described below, form the rules for our growth model.

Silicate polymers result from condensation⁶ of the hydrolyzed species produced by Eq. (4):



This reaction also proceeds by nucleophilic substitution above $\text{pH}=2$ and strongly favors reactions between highly condensed species [$R_k = (-\text{OSi})$] and monomers [$R_l = (-\text{OH})$ or $(-\text{OC}_2\text{H}_5)$]. In other words, growth proceeds by monomers attaching to clusters with reactions between clusters being impeded. This prejudice arises both because monomers most easily invert and because the preferred reaction is between the more acidic functional groups on the monomers and the more basic groups on the polymers.¹¹

From the above considerations, we can extract three basic rules of growth. (1) Polymers grow only from



FIG. 3. Typical cluster generated by poisoned Eden growth with an equal mixture of two- and four-functional monomers. The cluster contains 6400 sites. The plus signs represent growth sites. The surface fractal dimension, D_s , obtained from the radius dependence of the perimeter is 1.5 ± 0.1 , whereas the mass fractal dimension, D , obtained from the mass dependence of the radius, is 2.0 ± 0.1 .

monomers with all growth sites equally probable (reaction-limited nucleation and growth); (2) unhydrolyzed groups are permanently poisoned and bonds are never broken; (3) growth occurs from a fixed distribution of monomers of different functionalities. We believe that the mean functionality ($\langle n \rangle$) of the monomers and its variance are the most important variables. These parameters depend on the water concentration with the variance expected to be large because of the depletion of monomers of intermediate functionality. These growth rules are a variation of the Eden model.^{12,13}

In the Eden model, growth occurs on a lattice by addition of monomers to randomly chosen surface sites starting from a nucleus (seed). In our model, however, a fraction of the bonds is permanently poisoned according to rule (3) and subsequent growth occurs only on the unpoisoned or growth sites. Figure 3 shows a two-dimensional simulation grown from a 1:1 mixture of two- and four-functional monomers. The exterior surface of the resulting cluster is a fractal with a surface fractal dimension equal to 1.5 ± 0.1 . The rough structure is due to large spatial fluctuations in the density of growth sites resulting from the large variance in functionality. For certain monomer ratios growth eventually ceases because a statistical fluctuation in the number of low-functional monomers completely poisons the cluster.

Our observations imply the scattering behavior as a function of water concentration shown *schematically* in Fig. 4. At low water concentration (W small) corresponding to a low mean functionality and a large variance, the particles are mass fractals (at least at finite size), so that D , D_s , and the scattering exponent, P , are all equal. As the amount of water in the system increases (increasing $\langle n \rangle$ and decreasing its variance), D and D_s increase until they equal the dimension of space. At this point, the particle is insufficiently ramified to be considered mass-fractal, but has a maximally fractal surface. As W increases further, so many sites are available for polymerizations that the core of the

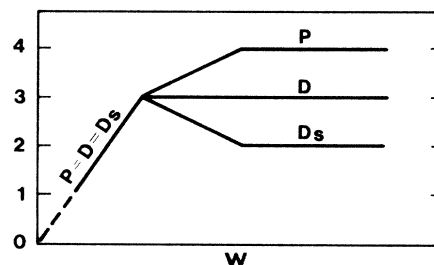


FIG. 4. Schematic trends expected for the mass (D) and surface (D_s) fractal dimensions as a function of W . The scattering exponent (P) is also included. Only the trends and crossover points are significant since we have no information on the actual shape of the curves.

particle becomes homogeneous ($D = d$), but, if the variance is large, the surface remains fractal with D_s decreasing from its maximum value of d . Finally, when the monomers are very highly hydrolyzed ($\langle n \rangle \rightarrow 4$ and its variance necessarily goes to zero), D_s reaches its minimum value of $d - 1$, D remains equal to d , and the scattering exponent reaches $d + 1$.

The full consequences of the above model are quite complex and have not been explored. We believe, nevertheless, that poisoned growth is the key idea needed to explain the observed structures. The model can generate uniform particles with fractally rough surfaces and the model displays the observed trends with W .

On the basis of the scattering data alone, we cannot exclude the possibility that the power-law scattering curves are due to polydispersity. If we have, for example, a distribution of uniform particles whose mass distribution, N , is a power law, $N(M) \sim M^{-\tau}$, then the exponent^{9,14} in the Porod regime is $-3(3 - \tau)$ for $\tau > \frac{5}{3}$. Depending on τ , the scattering exponent lies between 0 and -4 , consistent with the data. Within this interpretation the data in Fig. 1 imply that τ varies from 2.1 to 1.8 as W goes from 1 to 4.

It should be noted that the poisoned Eden model discussed above generates power-law size distributions under some conditions. In all cases where we observed such distributions, however, $\tau < \frac{5}{3}$ and so even within the model, polydispersity does not modify the interpretation presented here. Although our prejudice is to interpret the data in terms of a quasimonodisperse solution of rough particles, the distinction between such a system and a polydisperse collection of uniform particles is often academic. Surface-dependent properties (adsorption, catalysis, etc.), for example, should be identical for the two possibilities.

Pinhole SAXS data were taken under the supervision of J. S. Lin and S. Spooner at the National Center for Small Angle Scattering Research at Oak Ridge National Laboratory. This work was performed

at Sandia National Laboratories, Albuquerque, New Mexico and supported by the U. S. Department of Energy under Contract No. DE-AC-04-76DP00789, for the Office of Basic Energy Sciences, Division of Materials Sciences.

¹B. B. Mandelbrot, *Fractals, Form, Chance and Dimension* (Freeman, San Francisco, 1977).

²D. Avnir, D. Farin, and P. Pfeifer, *J. Colloid Interface Sci.* **103**, 112 (1985); A. J. Katz and A. H. Thompson, *Phys. Rev. Lett.* **54**, 1325 (1985).

³H. D. Bale and D. W. Schmidt, *Phys. Rev. Lett.* **53**, 596 (1984).

⁴D. W. Schaefer, J. E. Martin, A. J. Hurd, and K. D. Keefer, in *Physics of Finely Divided Matter*, edited by M. Daoud (Springer-Verlag, Berlin, 1985).

⁵D. W. Schaefer and K. D. Keefer, *Phys. Rev. Lett.* **53**, 1383 (1984).

⁶R. K. Iler, *The Chemistry of Silica* (Wiley, New York, 1979).

⁷S. H. Sinha, T. Freltoft, and J. Kjems, in *Kinetics of Aggregation and Gelation*, edited by F. Family and D. P. Landau (North-Holland, New York, 1984).

⁸D. W. Schaefer and K. D. Keefer, in *Better Ceramics Through Chemistry*, edited by C. J. Brinker, D. E. Clark, and D. R. Ulrich, Materials Research Society Symposia Proceedings Vol. 32 (North-Holland, New York, 1984), p. 1; D. W. Schaefer, J. E. Martin, and K. D. Keefer, *J. Phys. (Paris), Colloq.* **46**, C3-127 (1985).

⁹J. E. Martin, *J. Appl. Crystallogr.* **19**, 25 (1986).

¹⁰R. Aelion, A. Loebel, and F. Erich, *J. Am. Chem. Soc.* **72**, 5705 (1950).

¹¹K. D. Keefer, Ref. 8, p. 15.

¹²H. Eden, in *Proceedings of the Fourth Berkeley Symposium on Mathematics, Statistics, and Probability, 1960*, edited by Jerzy Neyman (Univ. of California Press, Berkeley, 1961), Vol. 4, p. 223.

¹³*On Growth and Form: Fractal and Non-Fractal Patterns in Physics*, edited by H. E. Stanley and N. Ostrowsky (Martinus-Nijhoff, Boston, 1985).

¹⁴P. W. Schmidt, *J. Appl. Crystallogr.* **15**, 567 (1982).